JOURNAL OF MATERIALS SCIENCE 29 (1994) 6199–6206

Creep behaviour and dislocation substructure evolution in the KBr–KI system

J. WOLFENSTINE, J.-H. SHIH
Materials Section, Department of Chemical Engineering, University of California, Irvine, CA 92717-2575, USA

Creep behaviour and dislocation substructure as a function of strain was investigated for two solid solution alloys and the pure components in the KBr–KI system. The creep characteristics for the KBr–KI alloys are in good agreement with creep behaviour observed in other ionic and class I metallic solid solution alloys, where the creep rate is controlled by a viscous dislocation glide process. The creep resistance of the KBr–KI alloys is higher than that for the pure components at the same value of homologous temperature. The dislocation substructure of the KBr–KI alloys and pure components at large strains consists of well defined subgrains. Subgrain formation is shifted to larger strains in the alloys compared to the pure components as a result of solute drag forces on dislocations during glide.

1. Introduction

Recently, the creep behaviour of two single crystalline ionic solid solution alloy systems KCl–RbCl [1, 2] and KCl–KBr [3, 4], which exhibit complete solid solubility over the entire composition range, has been investigated. Several important points were noted. First, the creep resistance of the ionic solid solution alloys was higher than that for the pure components at the same value of homologous temperature. Second, it was observed that the pure components (i.e. KCl) in both systems exhibited an extensive normal primary creep strain, stress exponent close to 5, nature of the creep transient after a stress reduction (the initial creep rate was slower than the steady state creep rate at the reduced stress), and well developed subgrains in the deformed samples whose size varied inversely with applied stress, suggesting that the creep behaviour of the pure components is similar to that exhibited by pure metals and class II metallic solid solution alloys and is controlled by a dislocation climb process. Third, a reduced primary stage compared to that for the pure materials, stress exponent close to 3, nature of the creep transient after a stress reduction (the initial creep rate was faster than the steady state creep rate at the reduced stress) exhibited by the solid solution alloys in both systems is in good agreement with creep behaviour observed in class I metallic solid solution alloys, where the creep rate is controlled by a viscous dislocation glide process. Fourth, the dislocation substructure for the solid solution alloys at large strains ($\varepsilon > 0.25$, where ε is true strain) consisted of well developed subgrains. For the case of the KCl–KBr alloys the dislocation substructure consisted of subgrains whose size was larger than that for the pure components at an equivalent value of normalized stress, σ/G, (where σ is the applied stress and G is the shear modulus) and varied inversely with applied stress. In contrast, the dislocation substructure observed in class I (glide control) metallic solid solution alloys is typically characterized by a random distribution of dislocations rather than well developed subgrains [5–10]. The above results suggest that the creep behaviour of ionic solid solution alloys is indeed similar to that observed in metallic solid solution alloys except for the nature of the dislocation substructure. In order to confirm this suggestion additional experimental data in other ionic solid solution alloy systems is required.

As a result, the present study was undertaken to investigate the creep behaviour in an additional ionic solid solution alloy system, KBr–KI, which also exhibits complete solid solubility over the entire composition range. In particular to:

1. observe how the creep resistance of the KBr–KI alloys compares to that for the pure components (KBr and KI) at the same value of homologous temperature;
2. compare the creep behaviour of the KBr–KI solid solution alloys with that exhibited by the KCl–KBr, KCl–RbCl and metallic solid solution alloys; and
3. investigate the nature of the dislocation substructure for the KBr–KI alloys as a function of stress and strain. At present results on the dislocation substructure for ionic solid solution alloys as a function of stress and strain exist only for the KCl–KBr alloys.

2. Experimental procedure

The KBr–KI system was chosen for the present study. The KBr–KI system exhibits complete solid solubility over the entire composition range [11]. Two solid solution alloys were selected:

1. KBr–47 mol % KI, [KBr(53)–KI(47)], and
2. KBr–25 mol % KI, [KBr(75)–KI(25)]. Single

0022–2461

crystals of these two compositions and pure KI were obtained from the Crystal Growth Laboratory, University of Utah. In addition, pure KBr single crystals were obtained from Solon Technologies Inc., OH. Spectrographic analysis revealed the total concentration of aliovalent cation impurities was less than 50 p.p.m. in each of the four different materials. The crystals were cleaved into {1 0 0} right parallelepipeds of approximately $4 \times 4 \times 8\ mm^3$. The specimens were polished to ensure the ends of the specimens were parallel to each other and perpendicular to the side faces.

The pure and solid solution alloy single crystals were deformed in uniaxial compression with the load applied along the ⟨1 0 0⟩ direction using the creep equipment and procedures previously described [1–4]. A majority of the creep experiments were performed at a single constant stress and temperature. All samples were annealed at the testing temperature in air for 2 h prior to testing. Samples were tested over the temperature range 640–700 °C at true stresses between 0.30 to 4.0 MPa in air. Samples were typically deformed to true strains between 0.2 to 0.4.

After completion of creep testing the samples were cooled rapidly under load to preserve the dislocation substructure formed during creep. The dislocation substructure was investigated using light optical microscopy on sections cleaved along {1 0 0} planes parallel to the applied stress axis. The cleaved samples were chemically etched at room temperature in a solution composed of 20 mg of $FeCl_3$ and 5 ml of glacial acetic acid in 25 ml of isoproponal.

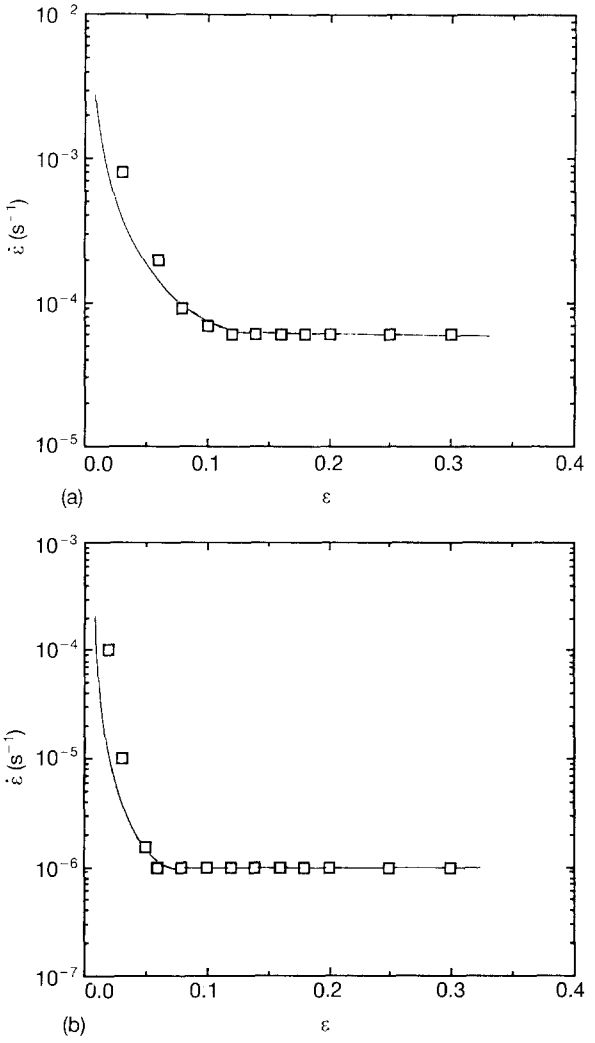

Figure 1 Strain rate versus strain for (a) KI at $T = 652\,°C$ and (b) KBr–47 mol % KI at $T = 640\,°C$. $\sigma = 0.5$ MPa.

3. Results

3.1. Creep curves

Representative creep curves for the pure components and alloys tested along a ⟨1 0 0⟩ direction are shown in Fig. 1. Fig. 1a is for KI and Fig. 1b is for the KBr(53)–KI(47) alloy. The data in Fig. 1 are plotted as logarithm of creep rate versus true strain. An examination of Fig. 1 reveals two important results. First, both KI and KBr(53)–KI(47) exhibit a normal primary creep stage, where the creep rate decreases with strain, followed by a steady state period in which the creep rate remains essentially constant. Pure KBr [3, 4] and KBr(75)–KI(25) also exhibit the same type of creep curve. Second, a primary creep strain of greater than 0.12 is required prior to the onset of steady state behaviour for KI. Pure KBr also required primary creep strains of at least 0.15 to achieve a steady state condition. The extent of the primary creep strain (≈ 0.06) for the KBr(53)–KI(47) alloy is less than that for pure KI. Normal primary creep strains of less than 0.07 were exhibited by KBr(75)–KI(25) prior to the onset of steady state behaviour. The length of the primary creep strain increased slightly at higher stress levels for both the pure components and the alloys. The extent of the primary creep strain for the alloys was always less than that exhibited by the pure components over the entire applied stress region investigated. The reduced primary creep strain for the two alloys compared to that for the pure components is consistent with behaviour observed in KCl–KBr [3, 4], KCl–RbCl [1, 2] and class I metallic solid solution alloys [5, 9, 12–19].

3.2. Stress dependence of the steady state creep rate

The dependence of the steady state creep rate on the applied stress for the KBr, KBr(75)–KI(25), KBr(53)–KI(47) and KI single crystals is shown in Fig. 2. All four materials were tested at about the same homologous temperature, $\approx 0.97\ T_m$, where T_m is the absolute melting temperature (KBr, $T = 973$ K, $T_m \approx 1007$ K; KBr(75)–KI(25), $T = 930$ K, $T_m \approx 959$ K; KBr(53)–KI(47), $T = 913$ K, $T_m \approx 941$ K; KI, $T = 925$ K, $T_m \approx 954$ K, where T is the absolute testing temperature [11]). The data in Fig. 2 are plotted as steady state creep rate, $\dot{\varepsilon}$, versus applied stress, σ, on a double logarithmic scale. An examination of Fig. 2 reveals four important results. First, both solid solution alloys have creep rates that are lower than those for both KBr and KI over the entire applied stress range. For example, at a given applied stress, the creep rates for both alloys are between 100 to 1000 times lower than those exhibited by the pure components.

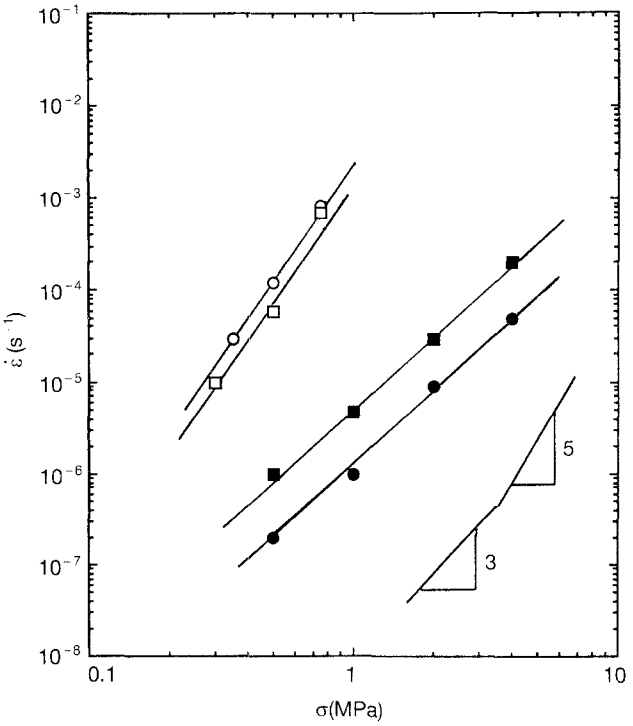

Figure 2 Steady state creep rate versus stress for (○) KBr, (□) KI, (■) KBr–47 mol % KI and (●) KBr–25 mol % KI tested at the same homologous temperature, $T/T_m = 0.97$.

Second, the creep rates for both KBr and KI are approximately equal. Third, the creep rates for the two alloys are different. At a given applied stress, the creep rate for KBr(75)–KI(25) is about a factor of 4 times faster than that for KBr(53)–KI(47). Fourth, the slope of the curves, the stress exponent, n, according to the relation, $\dot{\varepsilon} = k\sigma^n$, where k is a constant, is different for the alloys and pure components. The value of the stress exponent for the four materials as a function of composition is shown in Fig. 3. From Fig. 3 it is observed that the value of the stress exponent for KBr is 4.3 and 4.6 for KI. The values for KBr are in agreement with the previous results on both coarse grained and single crystalline KBr ($n \approx 4.3$–5.3) [20, 21]. At present no literature values are available for KI. The stress exponent for the KBr(75)–KI(25) alloy is 2.7. The stress exponent for the KBr(53)–KI(47) alloy is 2.6. The stress exponent for the two alloys is about the same. The decrease in the value of the stress exponent from 4.3 to 4.6 for KBr and KI to about 2.7 for the KBr(75)–KI(25) and KBr(53)–KI(47) alloys is in good agreement with behaviour observed in the KCl–NaCl [22], KCl–RbCl [1, 2] KCl–KBr [3, 4] ionic and Au–Ni [23] metallic solid solution alloy systems, where such a change has been attributed to a change in the rate-controlling creep mechanism from dislocation climb ($n \approx 4$–5) to viscous dislocation glide ($n \approx 3$).

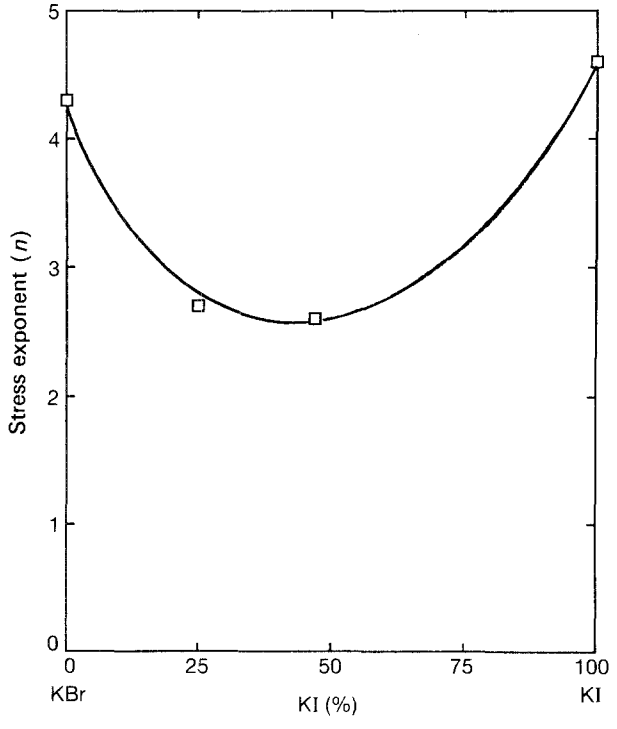

Figure 3 Stress exponent versus composition: $T/T_m = 0.97$.

3.3. Creep transient after a stress reduction

Stress reduction tests were conducted on KBr(75)–KI(25), KBr(53)–KI(47), KBr and KI. An example of a typical stress reduction test for (a) KI, and (b) KBr(75)–KI(25) is shown in Fig. 4. The data in Fig. 4 are plotted as logarithm of creep rate versus true strain. In both cases samples were deformed at a higher applied stress into the steady state region at which point the load is reduced (shown by the dashed line in Fig. 4), and the creep rate at the reduced stress as a function of strain is recorded until steady state behaviour is achieved at the lower applied stress level. From Fig. 4a, for the case of KI it is observed that the initial creep rate after the stress reduction from 0.50 to 0.30 MPa is slower than the steady state creep rate at the reduced stress of 0.30 MPa. Pure KBr exhibited a similar type of creep transient to that exhibited by KI [4]. The creep transient for KI and KBr is similar to that observed in pure metals and ionic solids (such as KCl) and class II metallic solid solution alloys, where dislocation climb is the rate-controlling process [1, 3, 5, 9, 12–19, 22]. In contrast, from Fig. 4b it is observed that the initial creep rate for KBr(75)–KI(25) after stress reduction from 1.0 to 0.5 MPa is higher than the steady state creep rate at 0.5 MPa. The KBr(53)–KI(47) alloy exhibited a similar type of creep transient to that displayed in Fig. 4b. The nature of the creep transient for the KBr–KI alloys is in good agreement with the behaviour observed in the KCl–NaCl, KCl–RbCl, KCl–KBr ionic and class I metallic solid solution systems, where dislocation glide is the rate-controlling process [1, 3, 5, 9, 12–19, 22].

3.4. Dislocation substructure

The dislocation substructure for the pure components and the alloys was investigated as a function of strain and stress. The effect of strain was investigated by examining the dislocation substructure in KI and KBr(53)–KI(47) at different points (values of strain) of the creep curves (constant stress) shown in Fig. 1.

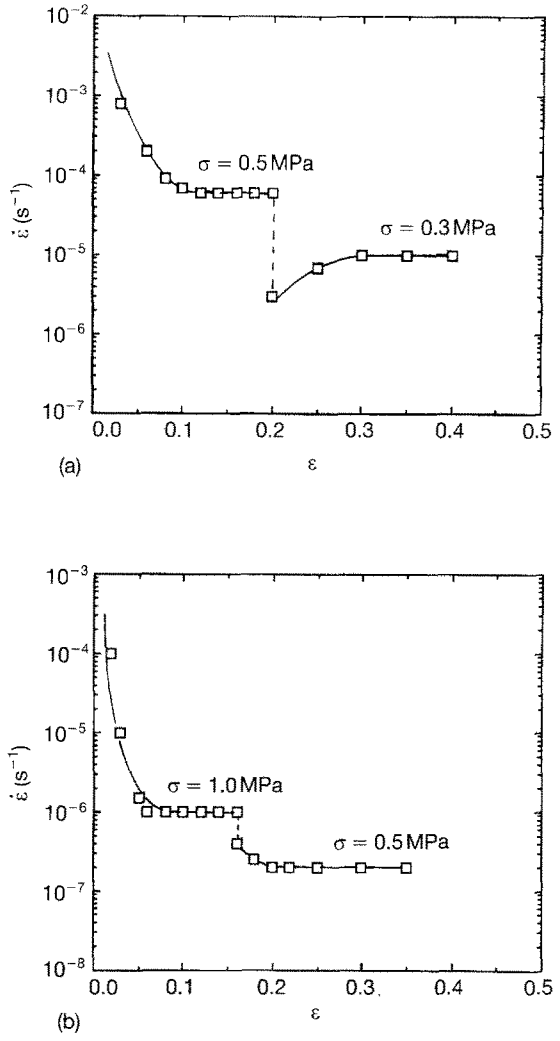

Figure 4 Stress reduction test for (a) KI at $T = 652\,°C$ and (b) KBr–25 mol % KI at $T = 657\,°C$.

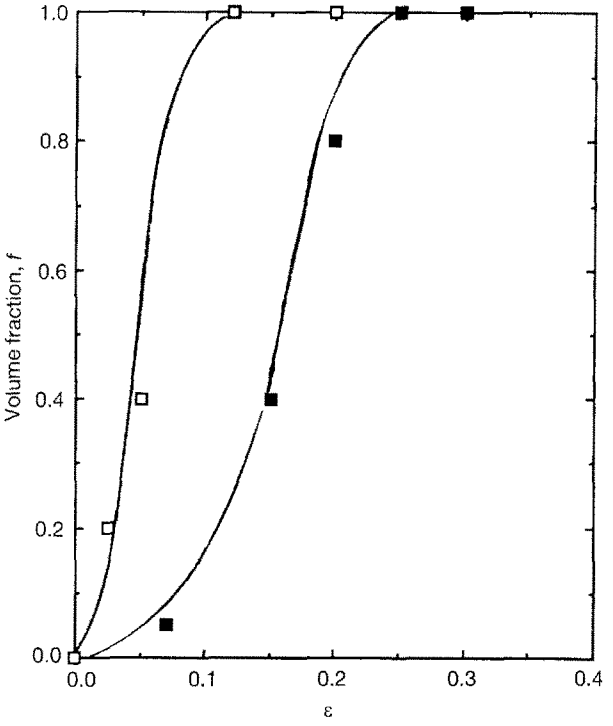

Figure 5 Volume fraction of material containing subgrains versus strain for (□) KI and (■) KBr–47 mol %: $T/T_m = 0.97$.

Prior to creep testing no subgrains were observed in KI and KBr(53)–KI(47). As strain accumulated, subgrain formation was observed in both KI and KBr(53)–KI(47). The volume fraction of material containing subgrains, f, as a function of strain is shown in Fig. 5. A value of $f = 1$ corresponds to a material completely filled with subgrains. From Fig. 5 several important points are noted. First, at large strains both materials exhibit a dislocation substructure of subgrains. An example of the dislocation substructure for KI and KBr(53)–KI(47) at large strains ($\varepsilon > 0.25$) is shown in Fig. 6a and b, respectively. Second, subgrain formation is retarded (shifted to larger strains) in the KBr(53)–KI(47) alloy compared to KI. For example, the strain required to reach $f = 1$ is greater in the KBr(53)–KI(47) alloy ($\varepsilon \approx 0.25$) than in KI ($\varepsilon \approx 0.12$). Third, the strain at which the creep rate for KI reaches essentially a steady state value ($\varepsilon \approx 0.12$) is the point at which the dislocation substructure approaches a volume fraction of subgrains equal to unity. For the case of the pure component the macroscopic (creep rate) and microscopic (subgrains) behaviours reach steady state at about the same value of strain. In contrast, for the KBr(53)–KI(47) alloy, the value of strain ($\varepsilon \approx 0.06$, Fig. 1b) at which point the creep rate reaches essentially a steady state value, the substructure consists of

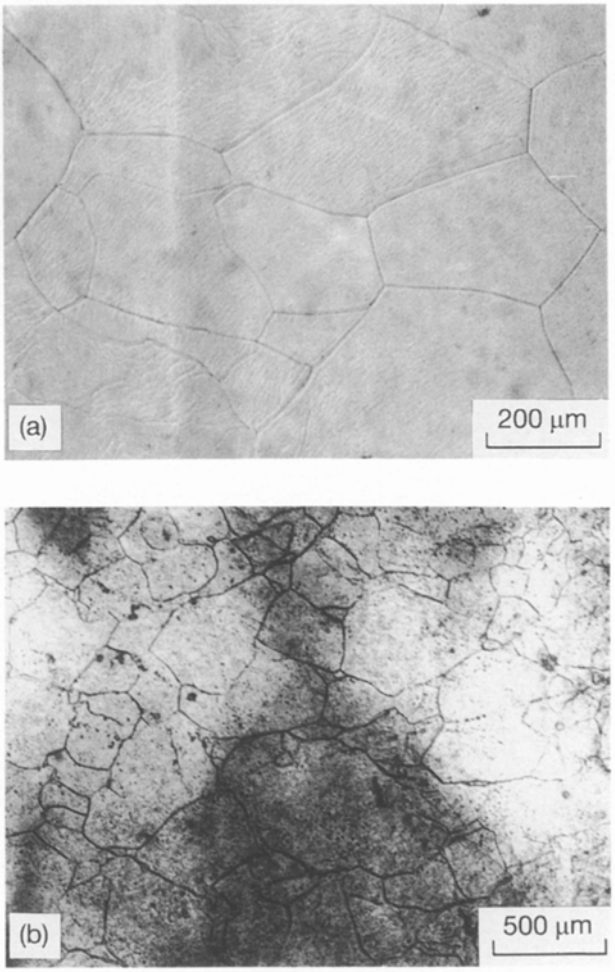

Figure 6 Dislocation substructure for (a) KI and (b) KBr–47 mol % at true strain equal to 0.25.

a random distribution of dislocations with little evidence for subgrain formation (< 5% subgrains). An example of the dislocation substructure at this point is shown in Fig. 7. It is important to note that the microscopic steady state for the alloy is one of the well developed subgrains (Fig. 6b). Thus, it appears for the case of the alloy that the macroscopic (creep rate) and microscopic behaviours (subgrains) do not reach steady state at about the same value of strain. Microscopic steady state is retarded compared to macroscopic steady state for the case of the alloy.

The effect of stress on the dislocation substructure was investigated for KBr, KBr(75)–KI(25), KBr(53)–KI(47) and KI at strains of greater than 0.25, where the substructure for all four materials consisted of well defined subgrains. No subgrains were observed in the two alloys, KBr and KI, prior to deformation. The subgrain size of the alloys and pure materials was determined as a function of applied stress at the same value of homologous temperature, 0.97 T_m. The subgrain size was measured using the linear intercept method. At least 150 subgrains were measured at each value of applied stress. The variation of the subgrain size, λ, with applied stress is shown in Fig. 8. The data in Fig. 8 are plotted as normalized subgrain size, λ/b, where b is the Burgers vector, versus normalized stress, σ/G, on a double logarithmic scale. The Burgers vector for: KBr = 4.66×10^{-10} m [24], KBr(75)–KI(25) = 4.75×10^{-10} m [25], KBr(53)–KI(47) = 4.82×10^{-10} m [25] and KI = 4.98×10^{-10} m [24]. Values of the shear modulus for the four materials were evaluated from the elastic constants using the relation [1, 26]

$$G = 3/5\, C_{44} + 1/5\, (C_{11} - C_{12}) \quad (1)$$

where C_{44}, C_{11} and C_{12} are the elastic constants. Values of the elastic constants for KBr [27] and KI [28] at the testing temperature were obtained from experimental data. Room temperature elastic constants for the KBr(75)–KI(25) and KBr(53)–KI(47) alloys are available [25]. The elastic constants at the testing temperature for the alloys were extrapolated from the room temperature data [29]. The shear modulus for: KBr = 4.68×10^3 MPa, KBr(75)–KI(25) = 4.24×10^3 MPa, KBr(53)–KI(47) = 3.96×10^3 MPa and KI = 3.43×10^3 MPa, at the testing temperatures given in Section 3.2. From Fig. 8 it can be observed that the subgrain size depends strongly on the applied stress for all four materials. The higher the applied stress, the smaller the subgrain size. The slope of the curve is about unity for both the pure components and the alloys. The subgrain size in the alloy is larger than that for the pure component at a given value of normalized stress (i.e. $\lambda_{KBr(75)-KI(25)} > \lambda_{KBr}$).

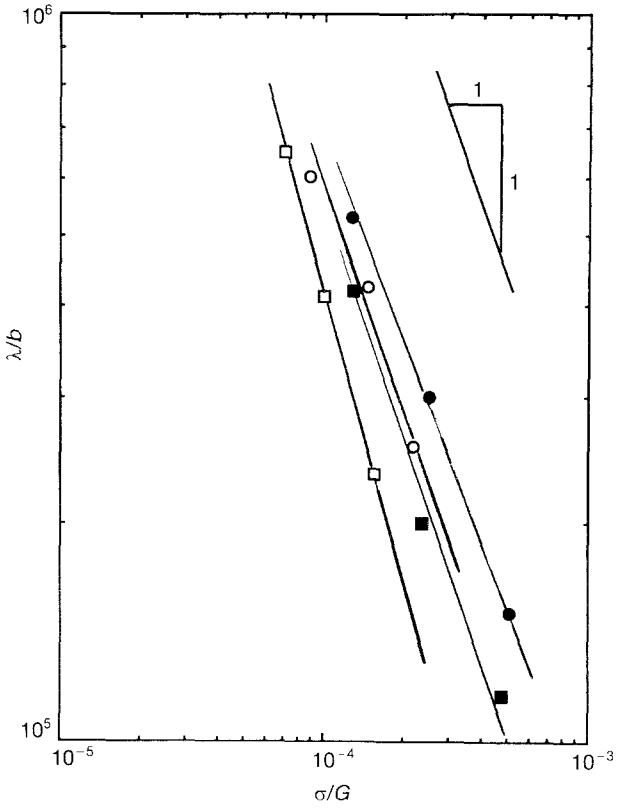

Figure 8 Normalized subgrain size versus normalized stress for (□) KBr, (○) KI, (●) KBr–47 mol % KI and (■) KBr–25 mol % KI: $T/T_m = 0.97$.

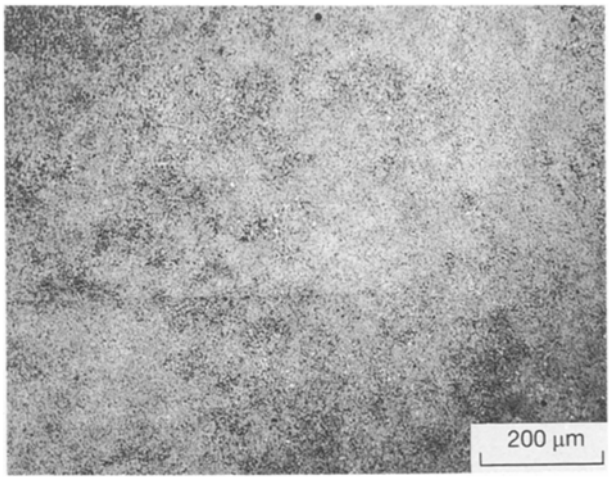

Figure 7 Dislocation substructure for KBr–47 mol % at true strain equal to 0.06.

4. Discussion

4.1. Comparison of the creep rate between the pure components and the alloys

From Fig. 2 it is observed that the creep rate for the alloys when compared to the pure components at the same homologous temperature ($\approx 0.97\ T_m$), reveals the creep resistance of the alloys is much greater than that for the pure components. This result is in agreement with the behaviour observed in the KCl–RbCl [1, 2] and KCl–KBr [2, 3] ionic solid solution alloy systems, where the alloys exhibited creep rates that were 20 to 1000 times lower than the pure components at a given value of applied stress when compared at the same homologous temperature. This result leads to an important point. It suggests the possibility of alloying coarse grained or single crystalline structural ceramics, such as sapphire (Al_2O_3) fibres which are

under consideration as potential reinforcements in oxide–oxide composites for use at temperatures above 1400 °C where creep resistance is an important variable [30, 31], as a method to increase the creep resistance of the composite. The creep resistance of a fibre composite is primarily determined by the creep resistance of the reinforcing fibres [31]. Thus, any mechanism which increases the creep resistance of the fibre will increase the creep resistance of the composite. Consequently, alloying for a structural oxide fibre such as Al_2O_3 with Cr_2O_3, which forms a complete solid solution over the entire composition range, can reduce the creep rate of the Al_2O_3 fibre and hence, the composite.

4.2. Class of creep behaviour

The creep characteristics of KBr and KI, including the value of the stress exponent ($n \approx 4$–5) length and shape of the primary creep curve (extended normal primary creep, $\varepsilon > 0.12$ to reach steady state), nature of creep transient after a stress reduction (the initial creep rate is slower than the steady state creep rate at the reduced stress) and character of the dislocation substructure after deformation (well developed subgrains whose size varies inversely with applied stress), suggests that the creep behaviour of KBr and KI is similar to that exhibited by pure metals, class II metallic solid solution alloys and other pure alkali halides where the rate-controlling mechanism is attributed to dislocation climb [12–19, 32–35]. More specifically subgrain data for the pure components KBr and KI, shown in Fig. 8, can be quantitatively compared to that for other pure alkali halides which develop well defined subgrains during creep. For pure alkali halides it is observed that the subgrain size varies with applied stress, according to the following relation [32, 33, 36]

$$\lambda/b = K(G/\sigma)^m \qquad (2)$$

where K and m are constants. For pure alkali halides the value of m is close to unity [32, 36]. For pure alkali halides K values between 2 to 210 have been reported [36]. The m and K values for KBr and KI determined from the data shown in Fig. 8 are 1.25 and 42, and 0.93 and 55, respectively. The results for KBr and KI are consistent with the data reported in other pure alkali halides.

The creep characteristics for the KBr(75)–KI(25) and KBr(53)–KI(47) alloys, including a stress exponent close to 3 versus 5 for the pure components, the reduced primary creep stage compared to the pure components and the results of the stress reduction tests (i.e. the initial creep rate after a stress reduction is faster than the steady state creep rate at the reduced stress) for the alloys is in good agreement with creep behaviour observed in KCl–NaCl [22], KCl–RbCl [1, 2], KCl–KBr [3, 4] ionic and class I metallic [5, 8, 12–19] solid solution alloys, where the creep rate is controlled by a viscous dislocation glide process.

For the case of the KCl–NaCl [22, 37], KCl–RbCl [1], KCl–KBr [4] ionic solid solution alloys it has been shown, as is the case in most class I metallic solid solution alloys, that the major force retarding dislocation glide is the dragging of solute ion atmospheres (Cottrell–Jaswon interaction [38]). For the case of viscous dislocation glide controlled by the dragging of solute atom (ion) atmospheres Mohamed and Langdon developed a criterion for predicting the type of creep behaviour (climb or glide) for a number of metallic solid solution alloys [5, 9, 15, 17, 37]. The criterion is based on the fact climb and glide are sequential mechanisms and, thus, the slower of the two is rate-controlling. It has been shown that the same criterion predicts the correct class of creep behaviour for the KCl–NaCl [37], KCl–RbCl [1] and KCl–KBr [4] solid solution alloys. The condition for a solid solution alloy to exhibit class I (glide) type of behaviour is given by [15, 37]

$$\frac{B\sigma^2}{k^2(1-v)}\left(\frac{\gamma}{Gb}\right)^3\left(\frac{D_c}{D_g}\right) > \frac{T^2}{e^2cb^6} \qquad (3)$$

where B is a dimensionless constant ($\approx 8 \times 10^{12}$), v is Poisson's ratio, D_g is the diffusion coefficient for glide, D_c is the coefficient for climb, e is the solute–solvent size difference, c is the concentration of solute, γ is the stacking fault energy, and k is the Boltzmann constant. It is of interest to examine whether the criterion given by Equation 3 can also correctly predict the type of creep behaviour (climb or glide) in the KBr–KI alloys. The applicability of Equation 3 to predict the creep behaviour in the KBr(75)–KI(25) and KBr(53)–KI(47) alloys is presented in the following section.

In order to apply Equation 3 to the case of the KBr(75)–KI(25) and KBr(53)–KI(47) alloys, v, D_g, D_c, e, c and γ for these alloys must be known. For the KBr(75)–KI(25) and KBr(53)–KI(47) alloys $c = 0.25$ and 0.47, respectively, with $e = 0.122$ and $v \approx 0.34$ for both alloys. At present no experimental data exists for D_g, D_c and γ for the alloys. The stacking fault energy for the alloys can be estimated from the stacking fault energy for KBr and KI using creep data as suggested by Mohamed and Langdon [39]. The normalized stacking fault energy, γ/Gb, for KBr is 3.0×10^{-2}. The normalized stacking fault energy, γ/Gb, for KI is 2.7×10^{-2}. Values for γ/Gb for the two KBr–KI alloys were obtained using a rule of mixtures [40]. The rule of mixtures yielded γ/Gb equal to 2.93×10^{-2} for KBr(75)–KI(25) and 2.86×10^{-2} for KBr(53)–KI(47). Since no data is available for D_c and D_g for the KBr(75)–KI(25) and KBr(53)–KI(47) alloys an estimate was made. It was previously shown that in a similar ionic solid solution system, KCl–KBr, where experimental data for D_c and D_g for the alloys was available, that the ratio of D_c/D_g was between 0.9 to 1.2 depending on the specific choice of D_c and D_g [4]. As a consequence of this result, in a first approximation the ratio for D_c/D_g for both the KBr(75)–KI(25) and KBr(53)–KI(47) alloys was set equal to unity.

Fig. 9 is a plot of $(kT/eGb^3)^2\ (1/c)$ versus $(\gamma/Gb)^3\ (D_c/D_g)\ (\sigma/G)^2$ on a double logarithmic scale. The solid line at 45° represents the criterion given by Equation 3 using $B = 8 \times 10^{12}$. This line separates the dislocation climb controlled creep behaviour on the

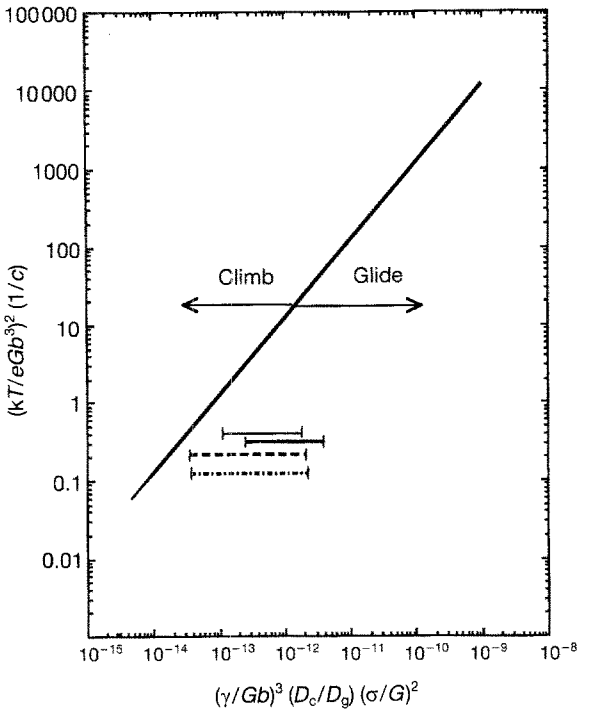

Figure 9 The glide–climb criterion represented by $(kT/eGb^3)^2$ $(1/c)$ versus $(\gamma/Gb)^3$ (D_c/D_g) $(\sigma/G)^2$ on a double logarithmic scale. The experimental results for the KBr–47 mol % KI (–.–.), KBr–25 mol % KI (– – –) and KCl–KBr solid solution alloys are shown: (———) KCl(70)–KBr(30), (———) KBr(67)–KCl(33).

left side from the dislocation glide controlled creep behaviour on the right side. Superimposed on Fig. 9 are two dashed horizontal lines representing the experimental conditions used for the KBr(75)–KI(25) and KBr(53)–KI(47) alloys. Also included in Fig. 9 are the experimental data for KCl–KBr alloys. From Fig. 9 it can be observed that the two dashed horizontal lines for the KBr–KI alloys fall on the right of the boundary, in agreement with the prediction of Equation 3 (glide control). This result adds further confirmation to the suggestion that the stress exponent of 3 and the other creep characteristics for the alloys presented earlier, are indeed a result of creep behaviour controlled by a viscous dislocation glide process. The results for the KBr–KI solid solution alloys also reveal that if the experimental conditions (i.e. applied stress is reduced) were changed slightly, that it may be possible to observe a change in creep behaviour for the alloys from control by glide to climb. At present no such transition has been reported in any ionic solid solution alloys. Current work is underway on the KBr–KI alloys to observe this transition in creep behaviour.

4.3. Dislocation substructure

The existence of subgrains in the KBr(53)–KI(47) and KBr(53)–KI(47) alloys is in agreement with the results for the KCl–KBr and KCl–RbCl alloys deformed to strains of 0.25 or greater [1, 2, 4]. It also has been recently reported that certain class I metallic solid solution alloys, Al–5 at % Mg [41–43], Fe–4.1 at % Mo [44] and Fe–6.3 at % Mo [45], deformed to large strains ($\varepsilon > 0.20$) in the $n \approx 3$ region exhibit a dislocation substructure consisting of well defined subgrains after deformation, rather than homogeneously distributed dislocations. For the case of the Al–5 at % Mg and KCl–KBr alloys it was observed that the subgrain size for the alloy varied inversely with applied stress, was larger than that for the pure material at a given value of normalized stress, σ/G, and subgrain formation in the alloys was shifted to higher strains compared to the pure components. These results are consistent with those exhibited by the KBr–KI alloys. The substructure observations for the ionic and metallic alloys are in agreement, suggesting similar creep behaviour between the two.

It is of interest to note that many of the typical class I metallic solid solution alloys, where the substructure consists of random dislocations, were in general deformed to strains of 0.10 or less [6–9]. In almost all of these alloys the creep rate (macroscopic) had reached steady state behaviour. The substructure for the KBr–KI (Fig. 7), KCl–KBr [4] and Al–5 at % Mg [41–43] alloys at similar strains ($\varepsilon \approx 0.10$) where a steady state creep reached was achieved, also revealed a substructure consisting mostly of random homogeneous dislocations. However, the microscopic steady state behaviour for the KBr–KI, KCl–KBr and Al–5 at % Mg alloys is one consisting of well defined subgrains. The random dislocation distribution observed for these typical metallic class I solid solution alloys is not the steady state substructure. It is likely that given enough strain ($\varepsilon > 0.20$) these metallic alloys that exhibited random dislocations at $\varepsilon \approx 0.10$ will have a substructure of well defined subgrains.

The results of this study, combined with previous work, suggest that the microscopic steady state substructure for both the pure components and ionic and metallic alloys is one consisting of subgrains. Subgrain formation is shifted to larger strains in the alloys compared to the pure components as a result of solute drag forces on dislocations during glide.

5. Conclusions

1. The reduced primary creep stage, the value of the stress exponent ($n \approx 3$) compared with that for the pure components ($n \approx 5$) and the results of the stress reduction tests (i.e. the initial creep rate after a stress reduction is faster than the steady state creep rate at the reduced stress) for the KBr(75)–KI(25), KBr(53)–KI(47) alloys are in good agreement with creep behaviour observed in KCl–NaCl, KCl–RbCl, KCl–KBr ionic and class I metallic solid solution alloys where the creep rate is controlled by a viscous dislocation glide process.

2. The creep behaviour of the KBr–KI alloys agrees with the prediction of the glide–climb criterion for solid solution alloys, assuming that the major force retarding viscous dislocation glide is due to the dragging of solute ion atmospheres.

3. The creep resistance of the KBr–KI alloys is higher than that for pure components at the same value of homologous temperature.

4. The dislocation substructure of the KBr–KI alloys and pure components at large strains consists of well defined subgrains. The subgrain size for both the alloys and the pure components varies inversely with stress. The subgrain size for the alloys is larger than that for the pure components at an equivalent value of normalized stress. Subgrain formation is shifted to larger strains in the alloys compared to the pure components as a result of solute drag forces on dislocations during glide.

Acknowledgements

This work was supported in part by Lawrence Livermore National Laboratory under grant IGPP/LLNL No. 93–50.

References

1. H. DUONG, M. BEEMAN and J. WOLFENSTINE, *J. Amer. Ceram. Soc.* **76** (1993) 185.
2. H. DUONG, M. BEEMAN, R. J. McCLELLAND and J. WOLFENSTINE, *Scripta Metall. Mater.* **26** (1992) 1331.
3. J. WOLFENSTINE, H. K. KIM and R. J. McCLELLAND, *Mater. Lett.* **14** (1992) 237.
4. H. DUONG, M. BEEMAN and J. WOLFENSTINE, *Acta Metall. Mater.* **42** (1994) 1001.
5. H. OIKAWA and T. G. LANGDON, in "Creep Behaviour of Crystalline Solids", edited by B. Wilshire and R. W. Evans (Pineridge Press, Swansea, 1985) p. 33.
6. N. MATSUNO and H. OIKAWA, *Scripta Metall.* **15** (1981) 319.
7. P. YAVARI, F. A. MOHAMED and T. G. LANGDON, *Acta Metall.* **29** (1981) 1495.
8. R. HORIUCHI and M. OTSUKA, *Trans. Jpn. Inst. Met.* **13** (1971) 284.
9. T. G. LANGDON in "Dislocations and Properties of Real Materials" (The Institute of Metals, London, 1984) p. 221.
10. A. ORLOVA and J. CADEK, *Z. Metall.* **65** (1974) 200.
11. L. P. COOK and H. F. McMURDIE in "Phase Diagrams for Ceramists", Vol. VII (The American Ceramic Society, Westerville, OH, 1989) p. 494.
12. J. CADEK, "Creep in Metallic Materials" (Elsevier, New York, 1988) p. 160.
13. O. D. SHERBY and P. M. BURKE, *Prog. Mater. Sci.* **13** (1967) 325.
14. W. R. CANNON and O. D. SHERBY, *Metall. Trans.* **1** (1970) 1030.
15. F. A. MOHAMED and T. G. LANGDON, *Acta Metall.* **22** (1974) 779.
16. S. TAKEUCHI and A. S. ARGON, *J. Mater. Sci.* **11** (1976) 1542.
17. M. S. SOLIMAN and F. A. MOHAMED, *Metall. Trans. A* **15** (1984) 1893.
18. T. FANG, R. RAO KOLA and K. L. MURTY, *ibid*, **17** (1986) 1447.
19. M. PAHUTOVA and J. CADEK, *Phys. Status Solidi A* **56** (1979) 305.
20. P. YAVARI and T. G. LANGDON, in "Surfaces and Interfaces in Ceramic and Ceramic–Metal Systems", edited by J. A. Pask and A. G. Evans (Plenum, New York, 1981) p. 295.
21. J. MONTEMAJOR, R. GOMEZ-RAMIREZ and E. CARRILLO, *Phys. Status Solidi A* **38** (1976) 76.
22. W. R. CANNON and O. D. SHERBY, *J. Amer. Ceram. Soc.* **53** (1970) 346.
23. C. M. SELLARS and A. G. QUARRELL, *J. Inst. Metals* **90** (1961–62) 329.
24. R. M. DAVIDGE, "Mechanical Behaviour of Ceramics" (Cambridge University Press, 1979) p. 24.
25. U. C. SHRIVASTAVA, *J. Appl. Phys.* **51** (1980) 1510.
26. C. BALLAD PIERCE, *Phys. Rev.* **123** (161) 744.
27. O. D. SLAGE and H. A. McKINSTRY, *J. Appl. Phys.* **38** (1967) 437.
28. A. A. GURCHENOK and V. L. UL'YANOV, *Soviet Phys. J.* **28** (1985) 828.
29. O. D. SLAGE and H. A. McKINSTRY, *J. Appl. Phys.* **38** (1967) 446.
30. G. CORMAN, *Ceram. Eng. Sci. Proc.* **12** (1991) 1745.
31. E. L. COURTWRIGHT, *ibid.* **12** (1991) 1725.
32. W. R. CANNON and T. G. LANGDON, *J. Mater. Sci.* **23** (1988) 1.
33. A. H. CHOKSHI and T. G. LANGDON, *Mater. Sci. Technol.* **7** (1991) 577.
34. A. G. EVANS and T. G. LANGDON, *Prog. Mater. Sci.* **21** (1976) 171.
35. A. K. MUKHERJEE, J. E. BIRD and J. E. DORN, *Trans. Amer. Soc. Metals* **62** (1969) 155.
36. S. V. RAJ and G. M. PHARR, *Mater. Sci. Engng* **81** (1986) 217.
37. F. A. MOHAMED and T. G. LANGDON, *J. Amer. Ceram. Soc.* **58** (1975) 533.
38. A. H. COTTRELL and M. A. JASWON, *Proc. Royal Soc. A* **199** (1949) 104.
39. F. A. MOHAMED and T. G. LANGDON, *J. Appl. Phys.* **45** (1974) 1965.
40. F. A. MOHAMED and Y. K. KIM, *Scripta Metall.* **11** (1977) 879.
41. W. BLUM, in "Hot Deformation of Aluminium Alloys", edited by H. D. Merchant, J. G. Morris, T. G. Langdon and M. A. Zaidi (Metallurgical Society American Institute of Mining, Metallurgical and Petroleum Engineers, Warrendale, PA, 1991) p. 181.
42. W. BLUM and E. WECKERT, *Mater. Sci. Engng* **86** (1987) 145.
43. E. WECKERT and W. BLUM, in "Proceedings of the Seventh International Conference on the Strength of Metals and Alloys", edited by H. J. McQueen, J. P. Bailon, J. I. Dickson, J. J. Jonas and M. G. Akben (Pergamon Press, Oxford, 1985) p. 773.
44. H. OIKAWA, M. SAEKI and S. KARASHIMA, *Trans. Jpn. Inst. Metals.* **21** (1980) 309.
45. H. OIKAWA, K. KANEKO and S. HASEGAWA, *Scripta Metall.* **18** (1984) 393.

Received 1 September 1993
and accepted 10 May 1994